Rev. Mexicana Astron. Astrof., **23**, 19-43 (1992)

THE OPACITY PROJECT — COMPUTATION OF ATOMIC DATA

M.J. Seaton[1], C.J. Zeippen[2], J.A. Tully[3], A.K. Pradhan[4],
C. Mendoza[5], A. Hibbert[6] and K.A. Berrington[6]

RESUMEN. Se presenta una descripción general de los métodos que usaron los participantes del Proyecto de la Opacidad para producir grandes conjuntos de datos radiativos atómicos de precisión, seguida de algunos ejemplos ilustrativos de los resultados que se obtuvieron.

ABSTRACT. A general description is given of the methods used by the participants in the international Opacity Project to produce massive sets of accurate radiative atomic data, followed by some illustrative examples of results obtained.

Key words: ATOMIC PROCESSES - TRANSITION PROBABILITIES

1 General Description (Seaton)

1.1 The Opacity Project Team

The Opacity Project—which will be referred to as OP—is concerned with the calculation of radiative opacities for atomic systems, and related work in computing atomic data and equations of state. Table 1 lists participants in the OP team.

1.2 Chemical elements included

Table 2 lists the chemical elements included. The nuclear charge is Z and "AG abundances" are solar photosphere abundances from Anders and Grevesse (1989). Calculations of atomic data are made for all the elements in Table 2, in all ionisation stages. It is planned, later, to include nickel.

1.3 Methods used for the computation of atomic data

I will give a general description of the methods used in the atomic-physics work and six of my colleagues will give some examples of results obtained.

Let me first re-capitulate some basic ideas of atomic-structure theory.

- **The Central-Field (CF) model.** An electron in a central field has a wavefunction $\phi_{nlm} = Y_{lm}(\hat{\mathbf{r}})(1/r)P_{nl}(r)$.
- **Configurations.** A configuration is defined by a set of nl quantum numbers and has a a wavefunction $\Phi(\mathbf{x}_1, ..., \mathbf{x}_N)$ constructed using functions ϕ_{nlm} and anti-symmetrised in space-and-spin co-ordinates $\mathbf{x}_i = (\hat{\mathbf{r}}_i, \sigma_i)$.
- **Configuration Interaction (CI).** The wavefunctions are $\Psi_k = \sum_j \Phi_j c_{jk}$ with the coefficients c_{jk} such as to diagonalise $(\Psi_k|H|\Psi_{k'})$. In the OP work we use two codes for CI calculations: CIV3 of Hibbert (1975) and SUPERSTRUCTURE of Eissner and Nussbaumer (1969) and Nussbaumer and Storey (1978). Both include facilities for the optimisation of the radial functions $P_{nl}(r)$.
- **Close-Coupling (CC).** The wave functions are $\Psi = \mathcal{A}\sum_i \psi_i(\mathbf{x}_i, ..., \mathbf{x}_N)\theta_i(\mathbf{x}_{N+1})$ where ψ_i is a CI function for an N-electron "target" state, θ_i a function for an added electron and $\mathcal{A}$ an anti-symmetrisation operator.

[1]Dpt. of Physics and Astronomy, University College London.
[2]UPR 261 du CNRS et DAMAp, Observatoire de Paris.
[3]Observatoire de la Côte d'Azur.
[4]Dpt. of Astronomy, Ohio State University.
[5]IBM Venezuela Scientific Center; also Visiting Fellow, IVIC.
[6]Dpt. Appl. Math. Theor. Phys., The Queen's University of Belfast.

Table 1: The Opacity Project Team

Initials	Name	Affiliation	Contribution
KAB	K.A. Berrington	QUB	atomic data
PGB	P.G. Burke	QUB	atomic data
VMB	V.M. Burke	QUB	atomic data
KB	K. Butler	MUO	atomic data
WD	W. Däppen	USCA	equations of state
WE	W. Eissner	QUB	atomic data
JAF	J.A. Fernley	UCL and VILSPA	atomic data
AH	A. Hibbert	QUB	atomic data
DGH	D.G. Hummer	JILA and MUO	atomic data and equations of state
AEK	A.E. Kingston	QUB	atomic data
MLD	M. Le Dourneuf	OPM	atomic data
DJL	D.J. Lennon	QUB and MUO	atomic data
DL	Ding Luo	JILA	atomic data
CM	C. Mendoza	IBMV	atomic data
DM	D. Mihalas	UI and NCSA	equations of state and opacities
SNN	S.N. Nahar	OSU	atomic data
GP	G. Peach	UCL	atomic data
AKP	A.K. Pradhan	OSU	atomic data and opacities
HES	H.E. Saraph	UCL	atomic data
PMJS	P.M.J. Sawey	QUB	atomic data
MPS	M.P. Scott	QUB	atomic data
MJS	M.J. Seaton	UCL	atomic data and opacities
PJS	P.J. Storey	UCL	atomic data
KTT	K.T. Taylor	RHBNC	atomic data
JAT	J.A. Tully	OCA	atomic data
YY	Yu Yan	UI and NCSA	atomic data and opacities
CJZ	C.J. Zeippen	OPM	atomic data

Affiliations:- IBMV=IBM Venezuela; JILA=Joint Institute for Laboratory Astrophysics; MUO=Munich University Observatory; NCSA=National Center for Supercomputer Applications; OCA=Observatoire de la Côte d'Azur; OPM=Observatoire de Paris (Meudon); OSU=Ohio State University; QUB=Queen's University of Belfast; RHBNC=Royal Holloway and Bedford New College (London); UCL=University College London; UI=University of Illinois; USCA=University of Southern California, Los Angeles; VILSPA=Villafranca Satellite Tracking Station.

Table 2: Chemical elements included

Element	Z	Log(AG abundance)
H	1	12.00
He	2	10.99±0.035
C	6	8.56 ±0.04
N	7	8.05 ±0.04
O	8	8.93 ±0.035
Ne	10	8.09 ±0.10
Na	11	6.33 ±0.03
Mg	12	7.58 ±0.05
Al	13	6.47 ±0.07
Si	14	7.55 ±0.05
S	16	7.21 ±0.06
Ar	18	6.56 ±0.10
Ca	20	6.36 ±0.02
Fe	26	7.67 ±0.03

In the OP work (Berrington *et al.*, 1987) the CI and CC approaches are combined, the wave functions being

$$\Psi = \mathcal{A}\sum_i \psi_i\theta_i + \sum_j \Phi_j c_j. \quad (1)$$

The functions θ_i and coefficients c_j are optimised using R-matrix methods.

1.3.1 R-matrix methods

One first defines a radius $r = a$ such that the functions ψ_i and Φ_j are small for $r > a$. We define the *inner* region to be that with $r \leq a$ and the *outer* region that with $r \geq a$.

For the inner region, one first obtains functions $\Psi^{(n)}$ which satisfy non-physical boundary conditions taken, in practice, to be $\{d(r\theta_i^{(n)})/dr\}|_{r=a} = 0$. This is done on expanding the $\theta_i^{(n)}$ in terms of sets of basis functions satisfying the non-physical boundary conditions: when Buttle corrections are included the sets are, effectively, complete. For states of given symmetry (specified total angular momenta and parity, $SL\pi$), one matrix diagonalisation is required to obtain the functions $\Psi^{(n)}$.

For the outer region one obtains sets of functions $\Psi^{(outer)}$ satisfying physical boundary conditions in the limit of $r \to \infty$. Fast numerical techniques have been developed.

Finally one obtains the physical functions Ψ on matching, at $r = a$, linear combinations of the $\Psi^{(n)}$ to linear combination of the $\Psi^{(outer)}$. Having carried out the one matrix diagonalisation, this gives an efficient method to obtain functions for large numbers of physical states, both bound states and continuum states (final states for photoionisation).

1.3.2 Radiative data

We require radiative data for f-values (bound-bound transitions) and photoionisation (bound-free transitions).

Let **D** be the dipole operator. We require reduced matrix elements, $(\Psi_f||\mathbf{D}||\Psi_i)$, for transitions between initial states i and final states f. Contributions from the inner region are obtained as linear combinations of the reduced matrix elements $(\Psi^{(n')}||\mathbf{D}||\Psi^{(n)})$, and contributions from outer regions by fast numerical integrations.

1.3.3 Line profiles

We define *isolated* lines to be those with nl states non-degenerate, and *hydrogenic* lines those with nl degenerate. R-matrix methods have been used to calculate line-profile parameters for 42 isolated lines and the results obtained have

been used to derive an empirical formula used for all other isolated lines (Seaton, 1988). Methods used for hydrogenic lines are described by Seaton (1990).

1.4 Summary of R-matrix calculations

All initial atomic-physics calculations were made in a non-relativistic approximation. Consideration was later given to inclusion of fine structure in the opacity calculations. Effects of intermediate-coupling have yet to be considered.

A *complex* is defined by Layzer (1959) to be a set of states having the same set of principal quantum numbers, n. As one goes along an isoelectronic sequence (fixed number of electrons and variable Z), all states of the same complex become degenerate in the limit of Z large. In making calculations for more highly ionised systems we would like to include, as target states, all states of the ground complex of the target. In practice this was possible for all systems with $N \leq 12$ (where N is the number of electrons in the target) but not for all of the systems with $N > 12$.

Table 3 gives a complete summary of the OP atomic-data calculations made to date. The columns are: values of N and Z; who did the work (initials from Table 1); and target configurations included.

For $N = 1$ (hydrogenic targets giving helium-like ions) we used target states $1s$, $2s$, $2p$ augmented by pseudo-states $\overline{3p}$, $\overline{3d}$ taken to be such as to give exact polarizabilities for $1s$. This choice gives rather accurate energy levels, f-values and near-threshold photoionisation cross sections, but inclusion of the pseudo-states gives unphysical pseudo-resonances at higher energies (these have been eliminated in data finally used for the opacity calculations).

For $N = 2$ we use target states $1s^2$, $\overline{1s^2}$ from Thornbury and Hibbert (1987), where $\overline{1s^2}$ is a pseudo-state chosen to give accurate polarizabilities for $1s^2$. This, again, gives pseudo-resonances which have to be eliminated. A similar approximation is used for $N = 10$, with targets $2p^6$, $\overline{2p^6}$.

For $N = 3$ we include the ground-complex states $2s$, $2p$ and the states $3s$, $3p$, $3d$.

For $N = 4$ to 9 we include all states of the target ground complex, i.e. all states involving $2s$ and $2p$ electron. For $N = 5$, $Z = 6$ (i.e. C I) we also include $2s^2 3s$, $2s^2 3p$ which come below some of the states of the ground complex.

For $N = 11$ to 12 we include all states of the ground complex, together with some additional states.

A lot of configuration interaction is included in the R-matrix calculations. For photoionisation processes that leads to inclusion of large numbers of autoionisation resonances.

For systems with $N \leq 12$ our calculations should be of fairly high accuracy. We expect most of our calculated f-values to be more accurate than values currently available in the literature, with the exceptions only of a fairly small number of cases for which highly optimized calculations, or precision measurements, have been made. Similar accuracy is to be expected for the photoionisation cross sections.

The systems with $N > 12$ are much more difficult because they have ground states with outer $n = 3$ electrons (or even $n = 4$) giving large numbers of energy levels. It is evident from Table 3 that, for these systems, much more drastic approximations have been made.

1.5 PEC resonances

PEC resonances in photoionisation cross sections are due to photoexcitation of the core followed by autoionisation (Yu Yan and Seaton, 1987). A simple example is

$$2snl \rightarrow 2pnl \rightarrow 2s + \text{electron}$$

where $2pnl$ is an autoionising state lying above the $2s$ series limit.

1.6 Level identifications

We use level identifications of two types: $(C\ k)$; and $(T\ i\ nl)$. The states $(C\ k)$ belong to the ground complex of the $(N+1)$-electron system and the wave functions are dominated by the functions Φ_j in equation (1); those of type $(T\ i\ nl)$ are dominated by target states ψ_i and an outer electron θ_i with quantum number nl (in some cases, where there are large amounts of configuration interaction, it can be difficult to make meaningful unambiguous identifications).

1.7 Subsidiary calculations

Initial opacity calculations were made using the atomic data as described in §1.4 and Table 3. The results obtained were significantly larger than those from earlier work (for example, Cox and Tabor, 1976) but, for some temperatures and

Table 3: Summary of R-matrix calculations

N	Z	Who	Target configurations
1	All	JAF, MJS, KTT	$1s$, $2s$, $2p$, $\overline{3p}$, $\overline{3d}$
2	All	GP, HES, MJS	$1s^2$, $\overline{1s^2}$
3	All	JAT, MJS, KAB	$2s$, $2p$, $3s$, $3p$, $3d$
4	6 to 26	JAF, AH, AEK, MJS	$2s^2$, $2s2p$, $2p^2$
5	6	DL, AKP	$2s^22p$, $2s2p^2$, $2p^3$, $2s^23s$, $2s^23p$
5	7 to 26	DL, AKP	$2s^22p$, $2s2p^2$, $2p^3$
6	All	VMB, DJL	$2s^22p^2$, $2s2p^3$, $2p^4$
7	All	KB, CJZ	$2s^22p^3$, $2s2p^4$, $2p^5$
8	All	KB, CJZ	$2s^22p^4$, $2s2p^5$, $2p^6$
9	All	MPS	$2s^22p^5$, $2s2p^6$
10	All	KTT	$2p^6$, $\overline{2p^6}$
11	12	KB, CM, CJZ	$3s$, $3p$, $3d$, $4s$, $4p$, $4d$, $4f$, $5s$
11	13 to 26	KB, CM, CJZ	$3s$, $3p$, $3d$, $4s$, $4p$, $4d$, $4f$
12	13, 14	CM, WE, MLD, CJZ	$3s^2$, $3s3p$, $3p^2$, $3s3d$, $3s4s$, $3s4p$
12	16, 18, 20	CM, WE, MLD, CJZ	$3s^2$, $3s3p$, $3p^2$, $3s3d$
12	26	CM, WE, MLD, CJZ	$3s^2$, $3s3p$, $3p^2$, $3s3d$, $3p3d$, $3d^2$
13	14	AKP	$3s^23p$, $3s3p^2$, $3s^23d$, $3s^24s$, $3s^24p$
13	16 to 20	AKP	$3s^23p$, $3s3p^2$, $3s^23d$
13	26	CM	$3s^23p$, $3s3p^2$, $3s^23d$, $3p^3$
14	16 to 20	KB, CM, CJZ	$3s^23p^2$, $3s3p^3$, $3s^23p3d$
14	26	CM	$3s^23p^2$, $3s3p^3$
15	All	KB, CM, CJZ	$3s^23p^3$, $3s3p^4$
16	All	KB, CM, CJZ	$3s^23p^4$, $3s3p^5$
17	18, 20	KAB, AH, MPS, CM	$3s^23p^5$, $3s3p^6$
17	26	CM	$3s^23p^5$, $3s3p^6$, $3s^23p^43d$
18	20	KAB, AH, MPS	$3p^6$
18	26	PJS, KTT	$3s^23p^6$, $3s^23p^53d$, $3s3p^63d$
19	20	AH, MPS, KAB	$4s$, $3d$, $4p$
19	26	HES, PJS	$3s^23p^63d$, $3s^23p^53d^2$, $3s^23p^64s$, $3s^23p^64p$, $3s^23p^64d$, $3s3p^63d^2$, $3s^23p^64f$
20	26	CM	$3d^2$, $3d4s$
21	26	KB	$3d^3$, $3d^24s$
22	26	KAB, PMJS	$3d^4$
23	26	KAB, PMJS	$3d^5$
24	26	KAB, PMJS	$3d^6$
25	26	KAB, PMJS	$3d^64s$, $3d^7$, $3d^54s^2$, $3d^64p$

densities, smaller than those from the OPAL project (see Iglesias and Rogers, 1991). The latter discrepancies were found to be due mainly to our having an insufficient number of atomic levels for some of the more complicated systems.

For the opacity work it is important to have levels in approximately correct positions and to allow correctly, at least in a statistical sense, for multiplet splittings (dependencies on i and on $SL\pi$). In making subsidiary calculations we made use of data which had already been computed to obtain additional data which, statistically, should be of sufficient accuracy. The states from these subsidiary calculations are referred to as PLUS states.

As an example of a case for which PLUS calculations were required we consider $(Z, N) = (26, 14)$ (i.e. Fe XIII), for which we had included only those target states belonging to configurations $3s^2 3p^2$, $3s3p^3$ and hence obtained only 9 target states $(T\ i)$. On the other hand, we had included quite a lot of states Φ_j in the expansions (1) and therefore had most, if not all, of the important states $(C\ k)$. The procedure used for the PLUS states was as follows. From calculations for $(Z, N) = (26, 13)$ we obtain a lot of states $(T\ k)$ which correspond to target states for the 14-electron system, and hence give energies for target states which had not been included in the $(26, 14)$ calculations. The energy of a state $(T\ i\ nl)$ can be expressed as

$$E(T\ i\ nl) = E(T\ i) - (Z - N)^2/(n - \mu)^2 \qquad (2)$$

where μ is a quantum defect. The quantum defects are slowly-varying functions of n and are fairly insensitive to i and to $SL\pi$. For each value of l we considered all states $(T\ i\ SL\pi)$ for which R-matrix calculations had been made and obtained mean values $\mu(l)$ of $\mu(i\ nl\ SL\pi)$ and r.m.s. deviations $\sigma(l)$. Practically all values of μ were found to lie in the range $\mu(l) \pm 2\sigma(l)$. For the PLUS states we took the quantum defects to be $\mu(l) + (1 - 2R)2\sigma(l)$ where R is a random number in the range $0 \leq R \leq 1$.

When configuration-interaction effects are not important, the f-value $f(i\ n'l'\ SL'\pi',\ i\ nl\ SL\pi)$ can be expressed as the product of $f(n'l',\ nl)$ times a Racah factor for the coupling of l, l' to the orbital angular momentum of the target to give total angular momenta L, L'. Results from the R-matrix calculations were used to obtain mean values of $f(n'l',\ nl)$ (values very different from the mean, due to CI effects, were rejected). These were then used to obtain values of $f(i\ n'l'\ SL'\pi',\ i\ nl\ SL\pi)$ for the PLUS states. These were included in the opacity calculations reported at the meeting.

Further work is required on photoionisation from the PLUS states.

2 The Photoionisation of Neutral Oxygen (Zeippen)

2.1 Introduction

The aim of this section is to illustrate the kind of approximations we used to produce massive numbers of accurate photoionisation cross sections. The case selected is neutral oxygen. Indeed, in an isoelectronic sequence, the neutral or lowly-ionised members are almost always the most difficult to treat. Also, oxygen has eight electrons, which is not a small number, while the fact that the residual ion O^+ has a ground configuration containing a half-filled outer shell $(2p^3)$ adds some specific difficulty to the problem of building an accurate representation for the "target" (see, for example, Eissner and Zeippen, 1981). The work described in the present section was performed in close collaboration by Keith Butler at MUO and myself (Butler and Zeippen, 1990, 1991 and 1992).

Apart from the opacity problem, the photoionisation of neutral oxygen is also of importance in the interstellar medium and in nebulae. The delicate problem of the photoionisation from the ground state of oxygen has attracted a lot of attention from both theoreticians and experimentalists over a long period of time (see the review by Seaton (1987) who discusses at some length the many aspects of the question). The practical consequence of this for our present purposes is that we have a lot of data with which to compare our results. The most recent experimental work is by Samson and collaborators (Samson and Pareek, 1985; Angel and Samson, 1988) while there exists an extended calculation by a team at QUB (Bell *et al.*, 1989; Bell and Hibbert, 1990; Bell *et al.*, 1990). Both the Belfast team and the authors of the present work used the methods mentioned by Seaton in §1.3 of this paper. Suffice it here to concentrate on the physical model we used in our calculation and to compare a few typical results with the most recent theoretical and experimental findings, thus illustrating the degree of accuracy reached in the OP work.

2.2 The physical model

The wavefunctions for the residual ion O^+ were obtained with the help of the computer program SUPERSTRUCTURE (Eissner *et al.*, 1974) in a version due to Nussbaumer and Storey (1978). Note that the importance of CI effects is commented on by Hibbert in Section 6 of the present paper.

Table 4: O^+ target configurations

Spectroscopic	Correlation
$2s^22p^3$	$2s2p^3\overline{3d}$
$2s2p^4$	$2s^22p^2\overline{4f}$
$2p^5$	$2s^22p\overline{3d^2}$
	$2s^22p^2\overline{3d}$
	$2p^4\overline{3d}$

Table 5: O^+ term energies in Rydbergs

Term		Measured	Present
$2s^22p^3$	$^4S^o$	0.0	0.0
$2s^22p^3$	$^2D^o$	0.244392	0.251886
$2s^22p^3$	$^2P^o$	0.368782	0.386804
$2s2p^4$	^4P	1.092816	1.149848
$2s2p^4$	^2D	1.512702	1.593638
$2s2p^4$	^2S	1.783523	1.936122
$2s2p^4$	^2P	1.937761	2.047678
$2p^5$	$^2P^o$	2.868751	3.019740

2.2.1 The target ground complex

In conformity with the OP rule for isoelectronic sequences up to Ne, the first requirement was to include the eight states corresponding to the ground complex, i.e.

$$2s^22p^3\ ^4S^o,\ ^2D^o,\ ^2P^o;\ 2s2p^4\ ^4P,\ ^2D,\ ^2S,\ ^2P;\ 2p^5\ ^2P^o.$$

As stated above, the treatment of a half-filled outer shell like $2p^3$ is rather delicate. Based on past experience with np^3 shells (Butler and Zeippen, 1984; Zeippen, 1987; Zeippen *et al.*, 1987), the configuration basis set in Table 4 was selected. Note that all configurations include the closed shell $1s^2$. The configurations listed are divided in two categories: the physical or spectroscopic ones, giving rise to the 8 terms in the ground complex, and the correlation ones, included in the calculation to improve the target representation. After optimisation (see Butler and Zeippen, 1990), the term energies obtained were as shown in Table 5. It is seen that the agreement between the calculated term energies and the observed ones (Fawcett, 1975) is satisfactory. It would be possible to reduce further the discrepancy by enlarging the configuration basis set but the main limitation here is that the target description must remain of a reasonable size if one wants to keep the size of the CC calculation within manageable limits. Indeed, the OP computations for an isoelectronic sequence concern (for all abundant ions up to iron) all states of the form

$$[(\text{target state symmetry})\ nl]\ \text{total state symmetry}\ ,$$

with $n \leq 10$ and $l \leq 3$, all other cases being considered as hydrogenic. As mentioned by Butler and Zeippen (1990), the present degree of accuracy for the target term energies is better than or comparable to all previous studies.

It is generally advisable not to base one's estimate of the quality of a target representation on the accuracy of the calculated term energies only (in this respect, semi-empirical methods where parameters are adjusted through a fitting procedure of experimental term energies should be used with caution and preferably by experienced workers). A further argument in favour of our chosen target wavefunctions is provided by Butler and Zeippen (1990) who compared

Table 6: Experimental O^+ term energies (in cm^{-1})

Term		Energy
$2p^3$	$^4S^o$	0
	$^2D^o$	26816
	$^2P^o$	40467
$2s2p^4$	^4P	119920
	^2D	165991
$2s^22p^23s$	^4P	185417
	^2P	189023
$2s2p^4$	^2S	195710
$2s^22p^23p$	$^2S^o$	203942
	$^4D^o$	206906
$2s^22p^23s$	^2D	206972
$2s^22p^23p$	$^4P^o$	208438
	$^2D^o$	211641
	$^4S^o$	212162
$2s2p^4$	^2P	212636

the oscillator strengths calculated with SUPERSTRUCTURE for selected transitions in O^+ using the configurations listed in Table 4. They find satisfactory agreement with the most reliable theoretical or experimental results available in the literature, concluding that the present representation for O^+ is suitable as a basis for the CC calculation.

2.2.2 The $n = 3$ target states

One important point deserves to be mentioned here. In the case of O^+, some $n = 3$ states lie among the $n = 2$ states of the ground complex, as shown in Table 6 (from Moore, 1971). It can be seen that configurations $2s^22p^23s$ and $2s^22p^23p$ give rise to terms which lie lower than the highest $2s2p^4$ terms. The question is therefore whether or not to include those $n = 3$ states in the target representation. Unpublished tests conducted by Seaton, Storey and Zeippen at the beginning of this work had shown that it is extremely difficult to build a balanced representation of all the $n = 2$ states plus some of the extra $n = 3$ states (it is impossible, in practice, to construct reasonable wavefunctions describing all the $2p^3$, $2s2p^4$, $2s^22p^23s$ and $2s^22p^23p$ states). Furthermore, the size of the target representation rapidly becomes enormous and this would not allow one to perform the CC part of the calculation for all the required OP symmetries, due to the cost in CPU time and memory. Finally, when some of them were included in the calculation, the extra states did not seem to have an important effect on the final results. Those are the reasons why we restricted our target to the $n = 2$ complex. Note that this problem is specific to oxygen and does not affect other members of the isoelectronic sequence in which $n = 3$ states lie higher. As Bell *et al.* (1989) did include some $n = 3$ states (arising from $2p^23s$) in their work, it is all the more important to compare their data with the present ones.

2.3 The photoionisation cross sections

I shall restrict myself to a short discussion of the photoionisation of neutral oxygen from the three states in the $2p^4$ ground configuration and a comparison of our data with the theoretical results of Bell *et al.* (1989) and the experimental measurements of Samson and colleagues. A more complete account of other previous work can be found in Butler and Zeippen (1990).

2.3.1 The ^3P ground state

Figure 1 displays our cross section for the photoionisation from the ^3P ground state of oxygen. It is compared with the data by Samson and Pareek (1985), Angel and Samson (1988) and Bell *et al.* (1989). It can be seen that there is

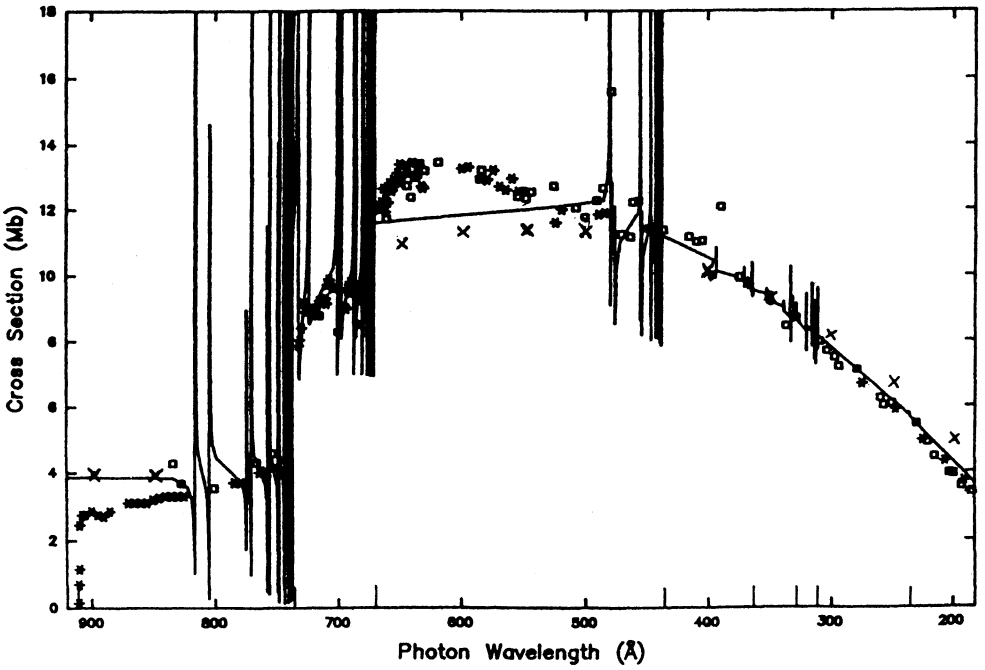

Figure 1: Total photoionisation cross section (in Mb) from the ^3P ground state of atomic oxygen as a function of the photon wavelength (in Å). Theory: full curve, present data; crosses, Bell *et al.*, 1989. Experiment: squares, Samson and Pareek (1985); stars, Angel and Samson (1988).

generally good agreement between the various sets of data. The figure shows that the experimental resonances and the present ones are very close to each other. Although not shown graphically, the discrepancy between the resonances of Bell *et al.* and ours is also very small. The overall agreement between the two theoretical cross sections is very good: over most of the photon wavelength range, they differ by less than 10 %. We note however that the discrepancy increases at lower wavelengths, where the present data is closer to experiment. The impression given by Figure 1 that our data are of high accuracy is confirmed by the more detailed analysis of Butler and Zeippen (1990), who take into account all recent calculations and experiments.

Unfortunately, there are two obvious differences with experiment: at threshold, the value of about 4.0 Mb produced by the two calculations is much larger than the 2.8 Mb measured by Angel and Samson (1988). There is no explanation for the discrepancy, as all recent close-coupling calculations yield cross sections close to 4.0 Mb at threshold and the previous experiment by Samson and Pareek (1985) also points to a value near 4.0 Mb. A more complete discussion can be found in Seaton (1987), Bell *et al.* (1989) and Butler and Zeippen (1990). To this day, the difference remains a small mystery.

The second discrepancy with experiment is linked with a more stable feature of measurements as both experiments by Samson and colleagues yielded a "peak" around 600 Å where all calculations give a "flat" cross section. Bell *et al.* suggest that contamination by molecular oxygen in the beam could be the culprit, and also note that the cross sections for the photoionisation from the first two excited states show a broad resonance precisely in the range around 600 Å (see below). Discussions with Samson have not yet permitted us to clear this second difficulty.

2.3.2 The ^1D and ^1S metastable states

Figures 2.a and 2.b show the present cross sections for the photoionisation of neutral oxygen from the first two ^1D and ^1S excited states, as compared with the data by Bell *et al.* It can be seen that the agreement between the two calculations is very good over most of the photon wavelength range. The discrepancy is generally less than 10 %.

2.4 The oscillator strengths

Although the present section of the paper is concerned with photoionisation, it is of interest to mention a few points concerning the OP oscillator strengths for oxygen. Indeed, the very philosophy of the techniques used is partly based on a similar treatment of bound-bound and bound-free transitions. Thus, the accuracy of our calculated oscillator strengths is an important element in assessing the quality of our work on photoionisation.

It would be useless to repeat the presentation of Butler and Zeippen (1991) or to anticipate the paper they are preparing for the "Atomic Data for Opacity Calculations" (ADOC) series in J. Phys. B (Butler and Zeippen, 1992). It should only be mentioned that for selected transition series, Butler and Zeippen (1991) find very good agreement with the most reliable experimental findings and with the most sophisticated theoretical results, particularly with the ones proposed by Bell and Hibbert (1990) using the same method and physical model as Bell *et al.* (1989). Each time the discrepancy between the two calculations becomes larger than 10 %, the present result appears to agree closer with experimental work or to be affected by a smaller discrepancy between the length and velocity values.

Furthermore, a recent study by Hibbert *et al.* (1991) using the structure code CIV3 (Hibbert, 1975) shows very good agreement with the present oscillator strengths.

2.5 Conclusion

In view of the detailed comparisons carried out by Butler and Zeippen (1990, 1991 and 1992), it can be said with confidence that the present extended radiative data set for oxygen is of very high statistical accuracy and that it provides a reliable basis for opacity calculations and perhaps for many other astrophysical applications. The effect of neglecting the lower $n = 3$ target states in our work appears to be very small. It will however be interesting to test this impression a bit further when even more powerful computers become available.

3 Four–Electron Atomic Systems (Tully)

The scope of the OP work of Tully *et al.* (1990) greatly exceeds that of Tully *et al.* (1989) which was concerned solely with photoionisation of B^+ from the ground state. The codes used by Tully *et al.* (1989) differed in only minor respects from the OP ones and the results they obtained are essentially the same as those of Tully *et al.* (1990). In the OP work we generated wavefunctions for a large number of bound states pertaining to Be, B^+, F^{+5} and ions of all the cosmically abundant elements listed in Table 2. With these we then computed 1814 energy levels, 33030 oscillator strengths and 1554 cross sections for photoionisation from terms lying below the first ionisation threshold. In order to resolve the autoionisation resonances we used fine energy meshes, resulting in a total of 859570 stored cross-section values.

We now make some comparisons with experimental and theoretical work for bound–free and bound–bound transitions.

The only absolute photoionisation measurements in the Be sequence we know of are those by Jannitti *et al.* (1986) for singly ionised boron. In this experiment a plasma containing B^+ was produced by directing a laser beam onto a crystalline boron rod. The plasma was traversed by a smooth UV continuum which enabled the optical thickness $\tau(\lambda)$ of the medium to be measured in the wavelength range $\lambda = 400$Å to $\lambda = 1400$Å. Cross sections for photoionisation from the ground ($2s^2\ ^1$S) and metastable ($2s2p\ ^3$P^o) states were obtained by dividing $\tau(\lambda)$ by the appropriate column density of absorbing ions. The latter was determined from the line spectrum by using theoretical f-values from Markiewicz *et al.* (1981). In contrast to our f-values, these were derived by means of a single configuration approximation. The comparison in Table 7 shows that there are significant differences in the neighbourhood of the interloper levels $2p3l$ which were not accounted for by Markiewicz *et al.* (1981). Since the normalisation procedure used by Jannitti *et al.* (1986) depends essentially on transitions to high lying levels (n = 7,8,9) for which there is agreement between the two methods, at least in so far as transitions to the ^{1}P^o and ^{3}D levels are concerned, we feel that the absolute experimental cross sections are probably quite reliable. In their Table III, Jannitti *et al.* give results at wavelengths where the spectrum lines merge into the continuum (Jannitti and Tondello, private communication). It is important to allow for this since the cross sections vary a lot with wavelength, especially for ionisation from the ground state. We have therefore extrapolated the OP cross

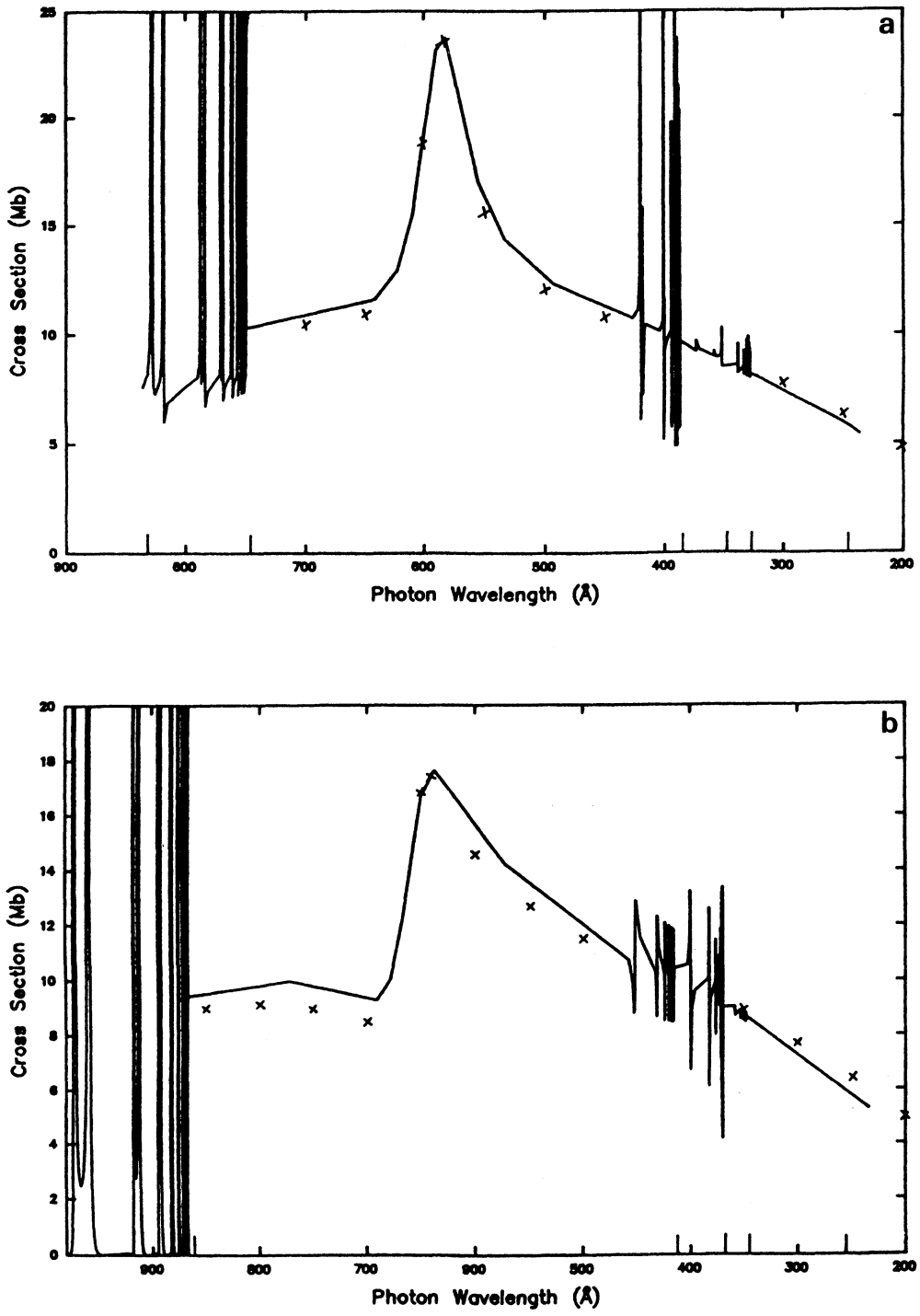

Figure 2: Total photoionisation cross sections (in Mb) from the ^1D (a) and ^1S (b) metastable states of atomic oxygen as a function of the photon wavelength (in Å). Theory: full curve, present data; crosses, Bell *et al.*, 1989.

Table 7: Comparing oscillator strengths for three Rydberg series in B^+. f-values are also given for transitions to the $2p3l$ interloper levels.

	$2s^2\ ^1S \rightarrow 2snp\ ^1P^o$		$2s2p\ ^3P^o \rightarrow 2sns\ ^3S$		$2s2p\ ^3P^o \rightarrow 2snd\ ^3D$	
n	f(PFC)	f(OP)	f(PFC)	f(OP)	f(PFC)	f(OP)
2	1.14	1.03				
3	5.47 (−2)	9.91 (−2)	6.13 (−2)	6.44 (−2)	4.51 (−1)	4.80 (−1)
4	2.92 (−2)	5.12 (−2)	1.0 (−2)	1.14 (−2)	1.16 (−1)	1.26 (−1)
5	1.51 (−2)	2.40 (−2)	3.7 (−3)	4.68 (−3)	4.9 (−2)	5.33 (−2)
$2p3s$	—	2.02 (−3)	—	—	—	—
6	8.7 (−3)	2.50 (−3)	2. (−3)	2.71 (−3)	2.5 (−2)	3.06 (−2)
$2p3p$	—	—	—	—	—	5.58 (−3)
7	5.4 (−3)	4.22 (−3)	1. (−3)	2.30 (−3)	1.5 (−2)	1.44 (−2)
$2p3p$	—	—	—	4.01 (−3)	—	—
8	4.0 (−3)	3.58 (−3)	7. (−4)	3.38 (−4)	1.0 (−2)	9.77 (−3)
9	2.7 (−3)⋆	2.77 (−3)		9.83 (−5)	7. (−3)⋆	6.76 (−3)

PFC: Polarized Frozen Core (Markiewicz *et al.* 1981)
OP: Opacity Project
⋆: Extrapolation by Jannitti *et al.* (1986)

sections below threshold to $n = 10$ before comparing. In this way we find that the experimental value for ionisation from the ground state is about 5% larger than theory (1.7 Mb as compared to 1.6 Mb), while for the metastable state the experimental result is about 20% smaller than ours (4.0 Mb as compared to 4.9 Mb). It is particularly satisfying to note that the magnitudes of the experimental cross sections are comparable with those of the Opacity Project. Furthermore, the resonances which Jannitti *et al.* observed and parameterised for photoionisation from the ground state closely resemble the behaviour predicted by OP theory. This happy agreement between theory and experiment has already been remarked upon by Tully *et al.* (1989).

Lang *et al.* (1987) have performed lifetime measurements for 6 transitions in N IV, 7 in O V and 2 in Ne VII. Six of their 15 A-values agree to better than 10% with ours. It is therefore puzzling to find that for seven transitions the measured A-values disagree with theory by factors varying from 1.5 to almost 6. On the other hand, there is excellent agreement for all of these transitions between our results and those from the multiconfiguration calculations by Laughlin *et al.* (1978), Glass (1979) and Hibbert (1980). Table 8 shows a comparison between the experimental and theoretical absorption oscillator strengths in N IV. OP wavelengths are included in the table and were used to derive f(Obs) from the observed A-values.

Tully *et al.* (1990) have compared some OP f-values with those from other approximations such as the one on which the well known CIV3 program (Hibbert 1975) is based. Here we draw attention to the extensive computations which B.C. Fawcett has performed to obtain energy levels and oscillator strengths for many atomic species. We make a few comparisons to illustrate the kind of agreement/disagreement that exists between his results and ours in the beryllium sequence. Fawcett's program allows for CI and has a Hamiltonian which includes both magnetic and electrostatic interactions. But unlike CIV3, it is not *ab initio*. Of particular interest is Fawcett's (1984) tabulation of gf-values for a variety of transitions in all ions from O V to Ni XXV, excepting Co XXIV. We consider the transitions $2s2p\ ^wP^o \rightarrow 2p3p\ ^wL$; $w = 1, 3$ and L = S,P,D. Fawcett's triplet data ($w = 3$) are presented alongside ours in Table 9. Whereas the OP results vary in a regular fashion along the sequence and tend smoothly up to hydrogenic values at $Z = \infty$, Fawcett's are approximately independent of Z. Occasionally they exhibit discontinuities, caused perhaps by subtle cancellation effects. For example, the fall in $gf(^3P^o \rightarrow {}^3P)$, which occurs between $Z = 20$ and $Z = 26$, can be traced to the behaviour of $gf(^3P^o_2 \rightarrow {}^3P_1)$. This increases from 0.19 ($Z = 12$) to 0.36 ($Z = 23$) and then falls abruptly to 0.011 ($Z = 24$), after which it again increases, reaching the value 0.096 ($Z = 28$). It can be seen that although Fawcett's $gf(^3P^o \rightarrow {}^3D)$ values differ substantially from ours (by almost a factor 2 at $Z = 12$), for the other triplet transitions there is reasonable agreement. However, for two of the singlet transitions there are striking differences between what Fawcett and the Opacity Project predict. Figure 3 is a plot of $gf(2s2p\ ^1P^o \rightarrow 2p3p\ ^1S$ and $^1P)$ against Z^{-1} for $Z \geq 12$. There is

Table 8: Comparing observed and theoretical oscillator strengths in N IV. Wavelengths in Å are from OP.

Transition	Wavelength	f(Obs)	f(OP)	f(CIV3)
$2s3p\ ^3\mathrm{P^o} \rightarrow 2s3d\ ^3\mathrm{D}$	7254.40	0.131	0.138	0.140
$2s2p\ ^3\mathrm{P^o} \rightarrow 2s3d\ ^3\mathrm{D}$	284.40	0.606	0.612	0.608
$2s3p\ ^1\mathrm{P^o} \rightarrow 2s3d\ ^1\mathrm{D}$	4039.30	0.346	0.274	0.260
$2s2p\ ^1\mathrm{P^o} \rightarrow 2s3d\ ^1\mathrm{D}$	338.05	0.485	0.524	0.565
$2s3s\ ^3\mathrm{S} \rightarrow 2s3p\ ^3\mathrm{P^o}$	3466.90	0.124	0.576	0.579
$2p^2\ ^3\mathrm{P} \rightarrow 2s3p\ ^3\mathrm{P^o}$	438.51	0.0025	0.0004	0.0004

Obs: Lang *et al.* (1987)
OP: Opacity Project
CIV3: Glass (1979)

Table 9: A comparison of $gf(2s2p\ ^3\mathrm{P^o} \rightarrow 2p3p\ ^3\mathrm{L})$ values for L = S,P,D.

	$gf(^3\mathrm{P^o} \rightarrow {}^3\mathrm{S})$		$gf(^3\mathrm{P^o} \rightarrow {}^3\mathrm{P})$		$gf(^3\mathrm{P^o} \rightarrow {}^3\mathrm{D})$	
Z	F	OP	F	OP	F	OP
12	0.343	0.240	1.026	0.747	1.405	0.722
13	0.339	0.245	1.033	0.791	1.274	0.762
14	0.342	0.256	1.064	0.829	1.267	0.797
16	0.331	0.268	1.086	0.891	1.264	0.854
18	0.313	0.278	1.077	0.938	1.277	0.899
20	0.284	0.286	1.056	0.976	1.331	0.935
26	0.331	0.302	0.794	1.054	1.471	1.012
∞		0.355		1.304		1.266

F: Fawcett (1984)
OP: Opacity Project

fair agreement for ^{1}S, but the way Fawcett's ^{1}P data points fall off as $Z^{-1} \rightarrow 0$ differs dramatically from the behaviour of our non-relativistic results. Fawcett's $gf(2s2p\ ^1\mathrm{P^o} \rightarrow 2p3p\ ^1\mathrm{D})$ values also decrease as Z increases (see Tully *et al.*, 1991). We note that this is confirmed by the intermediate-coupling calculations which Sampson *et al.* (1981) performed for $Z = 23$, 26 and 28. Of course since Fawcett makes allowance for relativistic effects his results will not necessarily tend to the same limit as ours at $Z = \infty$. According to Fawcett (1984) the intercombination transitions $^1\mathrm{P^o_1} \rightarrow {}^3\mathrm{P}_2$, $^3\mathrm{P}_1$ and $^3\mathrm{D}_1$ become important for $Z \geq 20$. It appears that a significant redistribution of certain oscillator strengths is occurring and this would explain why the transitions $^1\mathrm{P^o} \rightarrow {}^1\mathrm{P}$ and ^{1}D are less likely to occur in highly charged ions. As can be seen from Figure 3, the decrease in $gf(^1\mathrm{P^o} \rightarrow {}^1\mathrm{P})$ begins to manifest itself at values of Z much smaller than 20.

4 Photoionisation of Heavy Systems: Fe II (Pradhan)

The elements of the fourth row of the Periodic Table, and isoelectronic ions, are referred to as heavy systems within the present context. These require more extensive atomic calculations than lighter systems in terms of the necessary eigenfunctions needed to obtain an accurate and complete set of radiative parameters, oscillator strengths and photoionisation cross sections. One of the largest such calculations is being carried out for Fe II which is also of general astrophysical interest. An earlier, smaller set of calculations for Fe II has already been completed by Sawey and Berrington (1990). The present calculations employ a maximum of 45 LS states in the close coupling expansion for the e + Fe III → Fe II system dominated by electronic configurations $3d^6$, $3d^5 4s$ and $3d^5 4p$ of the target ion Fe III.

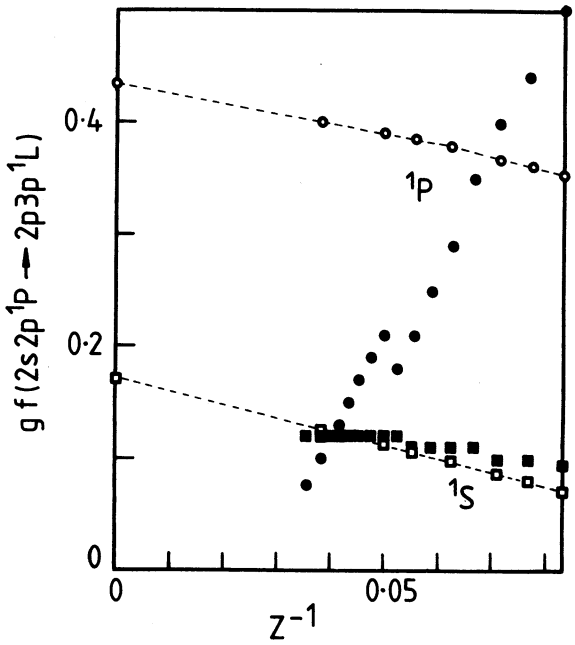

Figure 3: Variation of gf-values with atomic number Z. Open circles and squares, Opacity Project; filled circles and squares, Fawcett (1984).

The photoionisation cross sections for Fe II are significantly influenced by autoionisation resonances that arise due to the coupling between states included in the R-matrix calculations. In Figure 4 we present the ground state, $3d^6 4s\ ^6D$, cross section evaluated up to energies that cover the range of all the target states. The effect of the coupled target states manifests itself in two ways: (i) a rise in the background cross section and (ii) the resonance structures that further enhance the effective cross section. Details of the atomic physics calculations are described by Le Dourneuf *et al.* (1992).

In addition to the Rydberg type of resonances that converge on to series limits represented by the energies of the target states, there are also found to be another set of strong resonances associated with dipole allowed transitions within the ion core. These are the PEC resonances discussed in §1.5. An example of a PEC resonance in Fe II photoionisation is

$$3d^6(^5D)5d + h\nu \rightarrow 3d^5 4p(^5P^o)5d \rightarrow 3d^6(^5D) + e$$

where $h\nu$ is the photon energy equal to the energy between the core ion states of opposite parity ^5D and $^5P^o$, and the intermediate step represents a resonance state of the (e + Fe III) system with the excited Fe III core $^5P^o$. The valence electron, $5d$, does not play a strong role in the transition as it is weakly bound to the core states and therefore may be regarded as a "spectator", as in the dielectronic recombination process. The PEC resonances are thus found in the photoionisation cross sections of Rydberg-type bound states with an outer electron in an excited state. In Figure 5 we present cross sections for photoionisation of a series of Fe II states, $3d^6(^5D)nd\ ^6D$, where n ranges from 5 to 10. Some of the PEC features are clearly prominent in relation to other resonances and the background and are identified according to the excited core state of Fe III to which the resonance corresponds (the two $^5F^o$ states are non-degenerate states dominated by the configuration $3d^6 4p$ of Fe III).

An important inference to be drawn is that the photoionisation cross sections of apparently hydrogenic states (such as in Figure 5) may be greatly affected by the presence of PEC resonances and the excited states may have a considerably enhanced cross section compared to the hydrogenic approximation or other simple approximations such as the central field model.

5 Data Validation (Mendoza)

We describe here a series of comparisons and tests involving the OP atomic database that are being carried out in order to ensure data integrity. A more detailed account is given in Mendoza (1992).

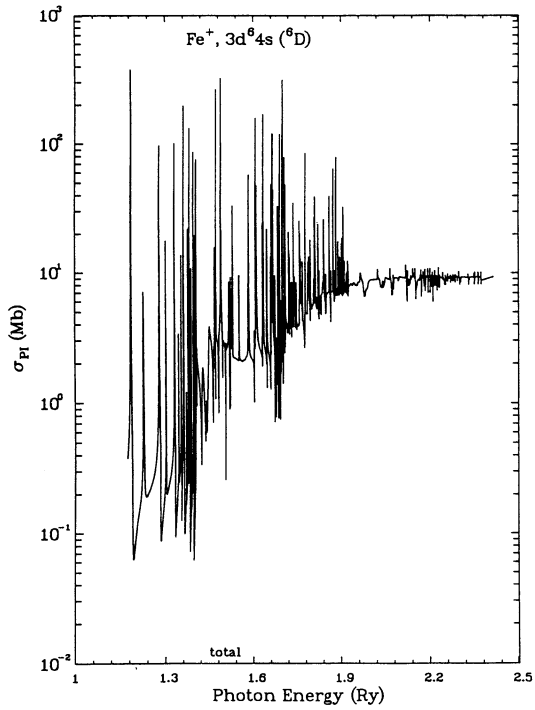

Figure 4: Photoionisation cross section of the ground state of Fe II.

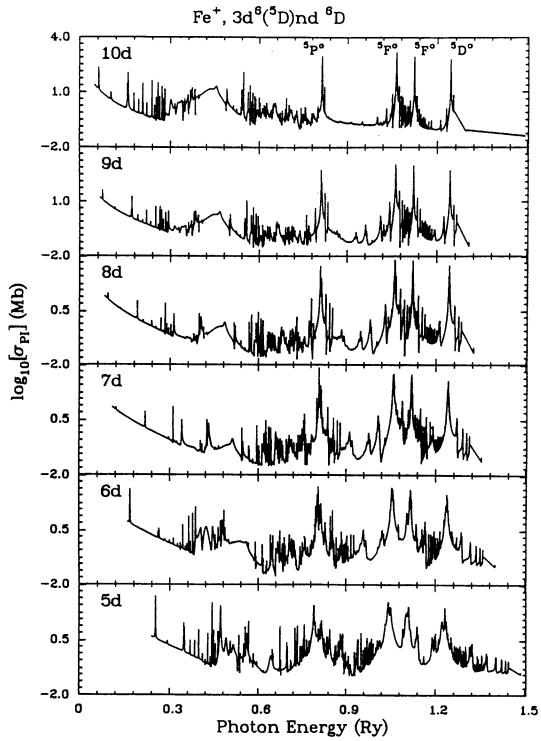

Figure 5: Photoionisation cross sections of bound states of Fe II in a Rydberg series showing PEC resonance features. On the Y-axis the values on the bottom and the middle of each panel correspond to the bound state denoted inside the panel; the values on top of the panels correspond to the next higher state.

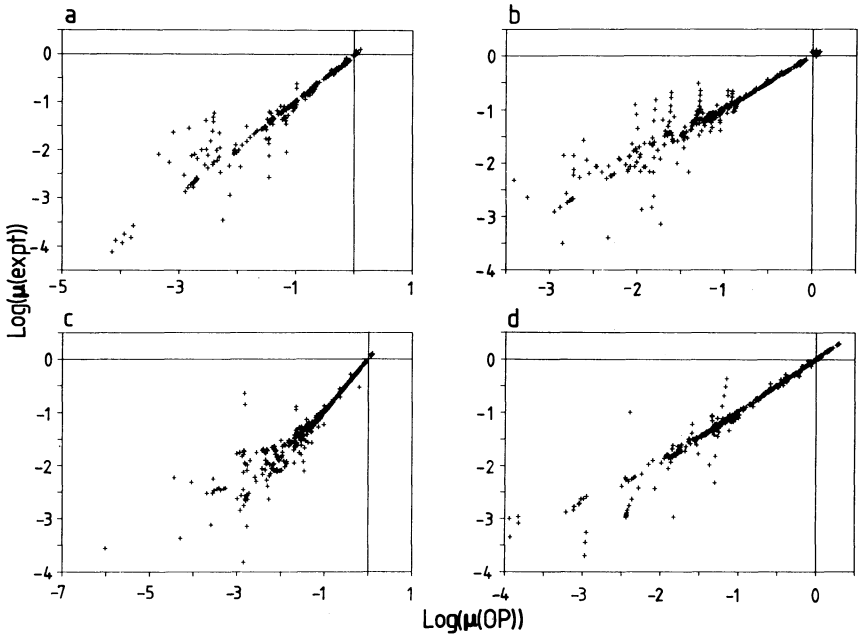

Figure 6: Log plots of measured quantum defects against OP values for non-hydrogenic ions of C, N, O and Si. (a) 317 states of C I - C V; (b) 467 states of N I - N VI; (c) 482 states of O I - O VII; (d) 491 states of Si I - Si XIII. References for experimental sources are given in Mendoza (1992).

5.1 Comparison with experimental energy levels

When possible we compare OP term energies and configuration assignments with those listed in spectroscopic tables. Mendoza (1992) presents such comparisons of OP quantum defects for non-hydrogenic ions of He, C, N, O and Si. The quantum defect $\mu(n)$ is defined by the expression

$$E(Tnl; SL\pi) = E(T) - z^2/[n - \mu(n)]^2 \quad (3)$$

where $E(Tnl; SL\pi)$ is the term energy in Ryd., $E(T)$ is the energy of the series limit and z is the effective ionic charge. The quantum defect gives a sensitive measure of the departure of a state from the hydrogenic energy position. In Figure 6, OP quantum defects for ions of C, N, O and Si are compared with experiment. It is found that the ratio of the number of measured states to the number of computed states decreases rapidly from $\sim$ 45% for C and N ions to 36% and 15% for O and Si ions respectively. For states with fairly large quantum defects the agreement is very good; the large differences that may be found for states with very small quantum defects are unimportant as such states are virtually hydrogenic. Noticeable differences are found for the following special cases: (i) effects caused by breakdown of LS coupling (e.g., excited states of C I) that are of course not reproduced by the OP results; (ii) experimental inaccuracies that show up in the highly excited states of some spectroscopic series (e.g., $1snd\ ^1D$ states of He I and the $nd\ ^2D$ series of O VI) and (iii) strongly mixed states. Unambiguous term assignments in the latter situation can be difficult.

5.2 Length/velocity oscillator strength agreement and oscillator strength distributions

When elaborate methods are used to compute oscillator strengths, a comparison between results obtained in the length and velocity formulations is usually given as a measure of the consistency and accuracy of the adopted approximations. Since the OP f-value database typically contains a few thousand transitions for an ion, and taking into account that f-values may vary by orders of magnitude, an indicator of the level of correlation between the two formulations may be implemented in terms of an *average percentage difference* (Yu Yan *et al.*, 1987). If two datasets $\{a\}$ and $\{b\}$ are to be compared, an average percentage difference may be defined as

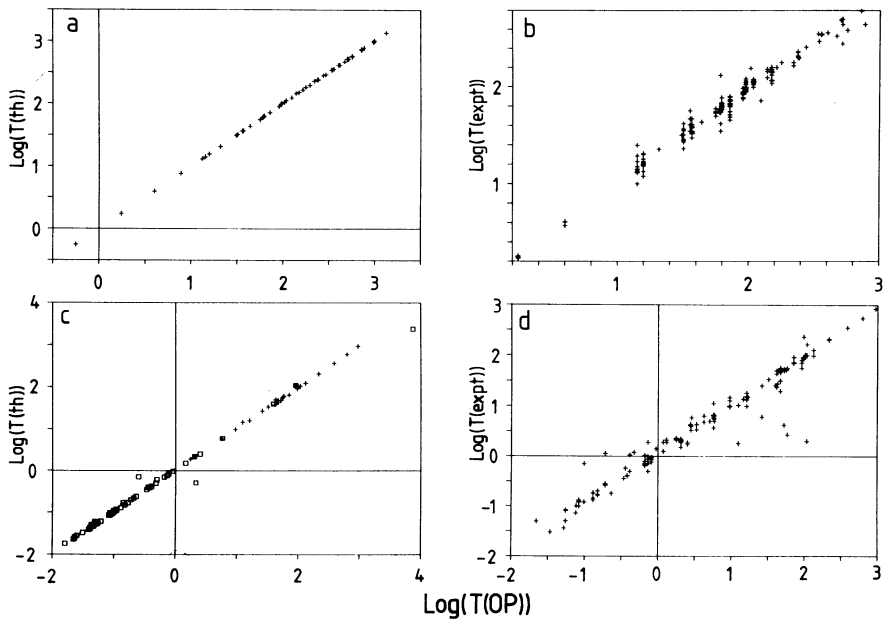

Figure 7: Comparison of OP radiative lifetimes for He I and Mg-like ions with experiment and theory. (a) Calculated values for He I by Theodosiou (1984). (b) Experimental lifetimes for He I compiled by Theodosiou. (c) Theoretical results for ions in the Mg sequence from Froese Fischer and Godefroid (1982) and Moccia and Spizzo (1988). (d) Measurements for Mg-like ions compiled by Butler *et al.* (1991). Lifetimes are given in ns.

$$\Delta(a,b) = 100 \times \left[\sum_i (a_i - b_i)^2\right]^{1/2} \left[\sum_i a_i \times b_i\right]^{-1/2} \tag{4}$$

For instance, it has been found that $\Delta(gf_l, gf_v) = 3.7\%$ for C II (Yu Yan *et al.*, 1987), where gf_l and gf_v are the length and velocity weighted oscillator strengths respectively, and that $\Delta(gf_l, gf_v) \leq 3\%$ for ions in the Mg isoelectronic sequence (Butler *et al.*, 1990). We have extended this test to the complete database and find that $\Delta(gf_l, gf_v)$ is usually much less than 10% for most species, except for ions of Fe with electron numbers $N_e > 14$ where differences as large as 26% are found. This is due to relatively simple target representations and large numbers of poorly correlated $n = 3$ bound-channel states (Mendoza, 1990).

A complete spectral distribution of oscillator strength is not only a requirement in opacity calculations but it is useful when inspecting the radiative properties of atomic states. For instance, the spectral distribution of oscillator strength of a state i obeys the sum rules

$$\sum_j f_{ij} + \int_0^\infty \frac{df}{d\epsilon} d\epsilon = N \tag{5}$$

$$\sum_j \frac{f_{ij}}{(E_j - E_i)^2} + \int_0^\infty \frac{1}{E^2} \frac{df}{d\epsilon} d\epsilon = \frac{\alpha}{4} \tag{6}$$

where N can be associated to the number of active electrons and α is the dipole polarizability of the state (here the polarizability is given in atomic units and energies in Rydberg units). These expressions allow consistency checks to be implemented on the radiative data and are indeed being used to examine the OP database.

5.3 Lifetime comparisons

Extensive comparisons of f-values and radiative lifetimes with available theoretical and experimental datasets are being made (see Mendoza 1992). For instance, in Figure 7, we compare OP lifetimes for He I and Mg-like ions with experiment and theoretical results. It can be seen that the correlation of the OP data with other theoretical results is at a much

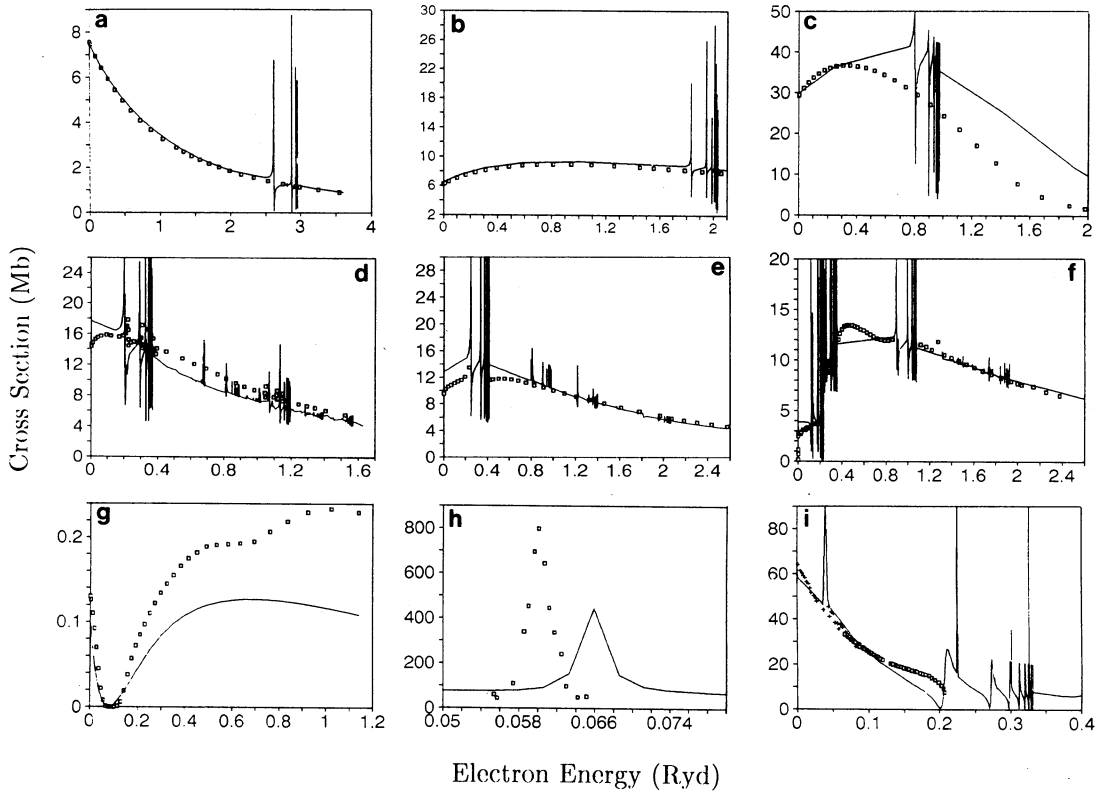

Figure 8: Comparison of OP photoionisation cross sections (solid curve) with experiment (squares and crosses). (a) He I ground state by West and Marr (1976); (b) Ne I ground state by West and Marr; (c) Ar I ground state by West and Marr; (d) C I ground state by Cantú *et al.* (1981); (e) N I ground state by Samson and Angel (1990); (f) O I ground state by Angel and Samson (1988); (g) Na I ground state by Hudson and Carter (1967); (h) $3s3p\ ^1P^0$ excited state of Mg I (Bradley *et al.* 1976); (i) Al I ground state by Kohl and Parkinson (1973) and Roig (1975).

higher level than with experiment. The r.m.s. deviations with the theoretical sets are 2% for He I and 8% for Mg-like ions. In the latter set we have excluded the very long-lived $3p^2\ ^1D$ state of Al II and the strongly mixed $3p3d\ ^1P^0$ and $3s6p\ ^1P^0$ states of Si III where large expected differences are encountered. On the other hand, the r.m.s. deviations with experiment are 19% and 22% for He I and Mg-like ions respectively (in the latter set we have excluded a few states with discrepancies larger than a factor of 2 that are most likely due to experimental problems). The poorer agreement with measurements, as discussed by Mendoza (1992), is believed to be due to difficulties inherent to experimental work, particularly in estimating cascade effects.

5.4 Comparison of photoionisation cross sections

We compare OP photoionisation cross sections with available absolute measurements, which are mainly for the ground state of neutrals. A representative set is shown in Figure 8. The agreement is found to be very good except in the high-energy region of the ground-state cross sections of Na I and Ar I. The discrepancy in the cross section of Na I is believed to be due to experimental error. An interesting case is the cross section of the $3s3p\ ^1P^0$ excited state of Mg I (see Figure 8). As shown, the cross section in the near-threshold region is dominated by a broad resonance identified with the $3p^2\ ^1S$ state. The OP position and width for this resonance are in poor agreement with experiment, and the cause of this discrepancy, found in other CC calculations, is not altogether clear.

We have also compared OP cross sections with the the systematic calculations for ground-state cross sections of positive ions by Reilman and Manson (1979). It is found that their cross sections agree fairly well with the OP background cross sections, but they do not obtain the resonance structure due to the neglect of correlation effects. The agreement begins to deteriorate for low stages of ionisation and neutrals.

Table 10: Some alternative ways of optimising radial functions in O V

	Case A	Case B	Case C
nl	Configurations used in optimisation		
$1s$, $2s$, $2p$	$2s2p\ ^3P^o$	$2s2p\ ^1P^o$	$2s2p\ ^1P^o$
$\overline{3s}$	$2s2p + 2p\overline{3s}\ ^1P^o$	$2s2p + 2p\overline{3s}\ ^3P^o$	$2s2p + 2p\overline{3s}\ ^3P^o$
$\overline{3p}$	$2s2p + 2s\overline{3p}\ ^1P^o$	$2s2p + 2s\overline{3p}\ ^3P^o$	$2p^2 + 2p\overline{3p} + \overline{3p^2}\ ^3P$
$\overline{3d}$	$2s2p + 2p\overline{3d}\ ^1P^o$	$2s2p + 2p\overline{3d}\ ^3P^o$	$2s2p + 2p\overline{3d}\ ^3P^o$
$\overline{4f}$	$2p^2 + 2p\overline{4f}\ ^1D$	$2p^2 + 2p\overline{4f}\ ^1D$	$2p^2 + 2p\overline{4f}\ ^1D$
Energies (a.u.)			Experiment[a]
$2s^2\ ^1S$	0.0000	0.0000	0.0000	0.0000
$2s2p\ ^3P^o$	0.3733	0.3744	0.3738	0.3747
$2s2p\ ^1P^o$	0.7334	0.7302	0.7296	0.7235
$2p^2\ ^3P$	0.9774	0.9782	0.9751	0.9739
$2p^2\ ^1D$	1.0628	1.0644	1.0580	1.0558
$2p^2\ ^1S$	1.3311	1.3317	1.3221	1.3118

Oscillator Strengths	f_l	f_v	f_l	f_v	f_l	f_v	Hibbert (1974) f_l	Hibbert (1974) f_v
$2s^2\ ^1S$ - $2s2p\ ^1P^o$	0.528	0.596	0.522	0.489	0.516	0.531	0.519	0.521
$2s2p\ ^1P^o$ - $2p^2\ ^1D$	0.157	0.167	0.157	0.108	0.158	0.155	0.158	0.152
$2s2p\ ^1P^o$ - $2p^2\ ^1S$	0.118	0.124	0.116	0.114	0.115	0.124	0.116	0.125
$2s2p\ ^3P^o$ - $2p^2\ ^3P$	0.194	0.216	0.192	0.178	0.195	0.207	0.194	0.219

a : Bockasten and Johansson (1968)

6 Comments on Some Target-State Wavefunctions (Hibbert)

6.1 Introduction

The detailed forms of the target wavefunctions can have a significant influence on oscillator strengths and photoionisation cross sections. Here we highlight two situations where it is important to use good quality CI functions.

6.2 Target states in Be-like ions

It is well-known that single-configuration wavefunctions lead to inaccurate oscillator strengths for these ions (Nicolaides *et al.*, 1973). For our purposes, CI target state wave functions must be constructed from a common set of radial functions and from a relatively small number of configurations. It is perhaps less well-known just how sensitive a range of oscillator strengths can be to the choice of those radial functions.

For O V, the target states of interest are of the form $2s^2$, $2s2p$, $2p^2$. We wish to limit the orbitals to $1s$, $2s$, $2p$, $\overline{3s}$, $\overline{3p}$, $\overline{3d}$, $\overline{4f}$, where nl denotes a spectroscopic orbital and $\overline{nl}$ a correlation orbital. We show in Table 10 the effect of choosing these orbitals in different ways. The $\overline{3d}$ and $\overline{4f}$ orbitals are chosen to describe the same correlation effect for each of the three cases. The $1s$, $2s$, $2p$ radial functions are taken as the Hartree-Fock (HF) functions of either $2s2p\ ^3P^o$ or $2s2p\ ^1P^o$, with the $\overline{3s}$ and $\overline{3p}$ orbitals being used both to allow the possibility of different HF orbitals in different states and to include some more electron correlation. It can be seen from Table 10 that whereas energy separations and length forms of the oscillator strengths differ only slightly from case to case, the velocity form of the oscillator strengths

Table 11: Comparison of energies and oscillator strengths in Ar II

		SC	CI	Accurate
Configurations	$^2P^o$	$3s^23p^5$	$3s^23p^5$	
	^2S	$3s3p^6$	$3s3p^6$	
			$3s^23p^4\overline{3d}$	
	ΔE (a.u.)	0.6773	0.4706	0.4932[a]
	f_l	0.312	0.012	0.0112[b]
	f_v	0.194	0.0002	0.0112

a : Minnhagen (1963)
b : Hibbert and Hansen (1987)

varies much more. Particularly interesting is the way in which f_v for the $^1P^o$ - ^1D transition improves considerably from a quite poor value purely by changing the $\overline{3p}$ function (compare cases B and C), yet configurations involving $\overline{3p}$ have quite small coefficients in the CI wavefunction.

6.3 PEC resonances in Argon

In the case of Ar-like systems, PEC resonances of the form $3s3p^6nl$ appear in the photoionisation cross sections of excited states $3s^23p^5nl$ and are much stronger than other members of Rydberg series. The transition occurs essentially in the core : $3s^23p^5$ - $3s3p^6$, with the outer electron appearing as a spectator. The magnitude of the cross section is closely related to the magnitude of the $3s^23p^5\ ^2P^o$ - $3s3p^6\ ^2S$ oscillator strength, so that the target states must give this result accurately. We show in Table 11 two simple calculations of target states. In the first (SC), only one configuration is used for each state, with the radial functions taken as those of the HF approximation for the ground state. In the second (CI) calculation, the ground state is still represented by the HF approximation, but the ^2S state is represented by the CI wave function

$$\Psi(^2S) = 0.80268\Phi(3s3p^6) + 0.59641\Phi(3s^23p^4\overline{3d})$$

where $\overline{3d}$ is a correlation function, radially much more compact than the lowest member of the $3s^23p^4nd$ Rydberg series. With this ^2S wave function, Table 11 shows that the $^2P^o$ - ^2S oscillator strength is very considerably reduced from the SC result. Moreover, the length form is in close agreement with the accurate CI calculation of Hibbert and Hansen (1987).

The effect of using this simple CI wavefunction as a target state is shown in Figure 9. Here we plot the cross section of photoionisation from $3s^23p^5np\ ^1S$ terms ($n = 3, 6$) against the effective quantum number $\nu(^2S)$ defined by

$$\nu(^2S) = -z/[E - E(^2S)]^{\frac{1}{2}} \qquad (7)$$

where z is the residual charge on the final state ion, E is the photon energy (in Rydbergs) and $E(^2S)$ is the energy of the ^2S final state.

The PEC resonance is seen when the effective principal quantum number of the np electron equals $\nu(^2S)$. It appears at $n = 4$ as the strongest resonance, and moves to the right as n increases. A comparison of the two sets of graphs in Figure 9 shows that the magnitude of the PEC resonance is considerably reduced when the CI wavefunction is used - by almost an order of magnitude. This reduction is principally due to the reduced oscillator strength of the core transition. Hence a satisfactory CI representation of the target states is essential in obtaining good photoionisation cross sections.

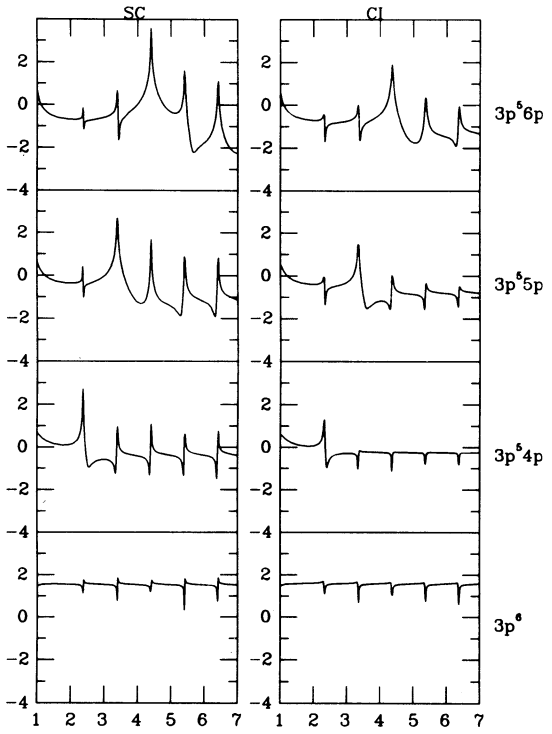

Figure 9: Resonances in the photoionisation cross section (in units of Log(Mb)) from Ar ^1S terms plotted against effective principal quantum number relative to ^2S.

7 Iron (Berrington)

7.1 Introduction

Opacity Project calculations for Fe, Fe^+, Fe^{2+} and Fe^{3+} were carried out by Sawey and Berrington (1990, 1992). It is interesting to highlight the results for Fe in order to see how far the computational techniques, which appear to give accurate data for light atoms and ions, can be applied to more complicated systems.

One immediate difficulty is that the lowest target terms (i.e. of Fe^+) are not in the same complex: the ground term configuration being $3d^64s$ while the first excited term is $3d^7$ (for readability, the closed shells $1s^22s^22p^63s^23p^6$ are omitted here). Computer time limitations prohibit the inclusion of, say, all $3d^64s$ and $3d^64p$ terms (there are 116). However, the $3d^6(^5D)$ core has a much lower energy than other $3d^6$ symmetries, so as a first approximation only $3d^6(^5D)4s$ and $3d^6(^5D)4p$ terms were included, which, together with the eight $3d^7$ terms and the low-lying $3d^5(^6S)4s^2$ term, make a total of 17 terms in the target expansion. Note that the $3d$ radial orbital is likely to be significantly different in these configurations, though no account for this is made in the present calculation.

A further problem is that relativistic effects are not negligible in iron. Again it would be a formidable computational challenge to include fine-structure levels explicitly (there are 54 levels associated with the above 17 terms); so, in keeping with what was done for lighter ions in the Opacity Project, the R-matrix calculation was performed in LS coupling (Sawey and Berrington, 1992).

7.2 The calculated bound terms for Fe

Fe term energies were calculated for even and odd parity LS terms having $L \leq 7$, $S \leq 3$ and $\nu \leq 10$, where ν is the effective principal quantum number relative to the lowest coupled ionisation threshold. This yielded 1023 terms, with 597 lying below the first ionisation threshold (the remaining terms are coupled to excited Fe^+ target states rather than to the ^6D ground state; such terms are bound in LS coupling). These calculated bound term energies are displayed in Figure 10 along with the lowest lying observed terms for comparison. In every case the calculated bound term lies higher in energy than the observed one, and this is a reflection of the limitations of the calculation.

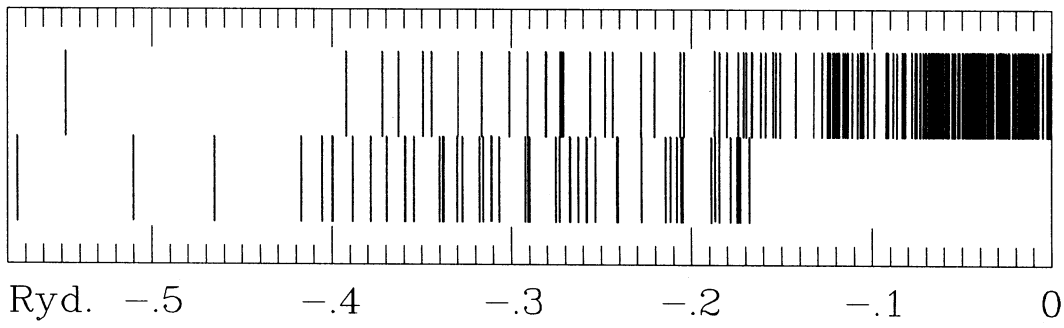

Figure 10: Fe term diagram displaying all calculated energies (above) and some corresponding observed energies (below) in Rydbergs relative to the first ionisation threshold.

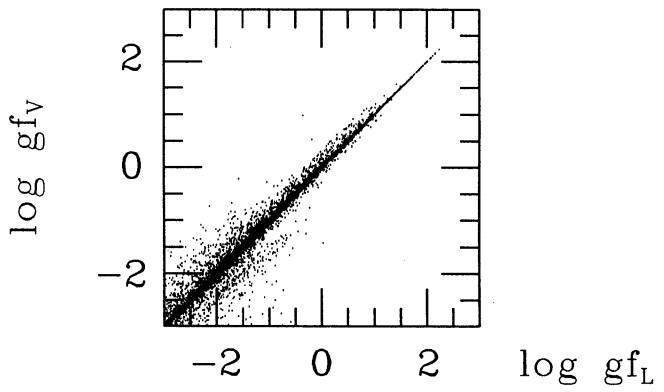

Figure 11: log gf_V plotted against log gf_L for transitions between all LS terms calculated for Fe.

7.3 The calculated gf-values for Fe

Weighted oscillator strengths were calculated for all dipole allowed transitions between all calculated bound terms. This yielded 27275 gf-values, of which 13419 are associated with terms lying below the first ionisation threshold. Two assessments are made here of the accuracy of these data.

Firstly, a comparison can be made of the length and velocity forms of the calculated gf-values, to give some indication of the self-consistency of the wavefunction. Figure 11 shows the log of the velocity form of each gf-value plotted against the log of the length form. Perfect length/velocity agreement would be denoted by each point lying on a straight diagonal line on such a plot. Some scatter is evident, but agreement is reasonable especially for the values of larger magnitude.

Secondly, a small sample of individual gf-values are compared in Table 12 with those calculated by Fawcett (1987) and from the tabulation of Fuhr *et al.*(1988). Fawcett's calculations involve the optimisation of Slater parameters to minimise discrepancies in calculated and observed wavelengths. Fuhr *et al.*'s paper is essentially an assessment and compilation of both theoretical and experimental work; references to the original work are contained therein, but they rely mostly on experimental data, which is often of high accuracy for Fe. Both tabulations present gf-values for transitions between fine-structure levels, and the multiplet sum is shown here. The qualitative agreement with the OPACITY calculations for these transitions is good, though there are quantitative discrepancies.

Table 12: Calculated gf-values in LS coupling for Fe I compared with the tabulations of Fawcett (1987) and Fuhr *et al.* (1988) where available.

Configuration	Transition	Fawcett	Fuhr *et al.*	OPACITY
$3d^7(^4\mathrm{F})4s$ - $3d^6(^5\mathrm{D})4s4p(^3\mathrm{P}^o)$	$a^3\mathrm{F}$ - $z^3\mathrm{F}^o$	-	0.04	0.11
$3d^7(^4\mathrm{F})4s$ - $3d^7(^4\mathrm{F})4p$	$a^3\mathrm{F}$ - $y^3\mathrm{F}^o$	4.45	5.25	6.67
$3d^7(^4\mathrm{F})4s$ - $3d^6(^5\mathrm{D})4s4p(^3\mathrm{P}^o)$	$a^3\mathrm{F}$ - $z^3\mathrm{D}^o$	0.06	0.10	0.25
$3d^7(^4\mathrm{F})4s$ - $3d^7(^4\mathrm{F})4p$	$a^3\mathrm{F}$ - $y^3\mathrm{D}^o$	3.86	4.68	4.91
$3d^7(^4\mathrm{F})4s$ - $3d^7(^4\mathrm{F})4p$	$a^3\mathrm{F}$ - $z^3\mathrm{G}^o$	3.88	2.88	7.81
$3d^64s^2$ - $3d^6(^5\mathrm{D})4s4p(^3P^o)$	$a^5\mathrm{D}$ - $z^5\mathrm{D}^o$	0.55	0.57	0.55
$3d^64s^2$ - $3d^6(^5\mathrm{D})4s4p(^3P^o)$	$a^5\mathrm{D}$ - $z^5\mathrm{F}^o$	1.12	1.12	1.21
$3d^7(^4\mathrm{F})4s$ - $3d^7(^4\mathrm{F})4p$	$a^5\mathrm{F}$ - $z^5\mathrm{G}^o$	7.38	6.30	10.7
$3d^6(^5\mathrm{D})4s(^6\mathrm{D})4d$ - $3d^6(^5\mathrm{D})4s4p(^3\mathrm{P}^o)$	$f^7\mathrm{D}$ - $z^7\mathrm{F}^o$	-	0.56	0.21
$3d^6(^5\mathrm{D})4s(^6\mathrm{D})4d$ - $3d^6(^5\mathrm{D})4s4p(^3\mathrm{P}^o)$	$e^7\mathrm{F}$ - $z^7\mathrm{D}^o$	-	4.29	2.58
$3d^6(^5\mathrm{D})4s(^6\mathrm{D})4d$ - $3d^6(^5\mathrm{D})4s4p(^3\mathrm{P}^o)$	$e^7\mathrm{F}$ - $z^7\mathrm{F}^o$	-	1.98	1.09

7.4 The calculated photoionisation cross sections for Fe

The photon-energy dependent total cross section for photoionisation was calculated for all bound terms with $L \leq 6$ lying below the first ionisation threshold. A sufficiently fine energy mesh was used in order to delineate the autoionising resonances occuring below each coupled ionisation threshold included in the target state expansion.

Figure 12 shows the calculated photoionisation cross section from the two lowest ^7S excited states of iron; these plots illustrating well the effect of PEC resonances. The mechanism for formation of the intermediate autoionisation state which gives rise to PEC resonances here is

$$h\nu + 3d^6(^5D)4s(^6D)nd\ ^7S \rightarrow 3d^6(^5D)4p(^6D^o, ^6F^o, ^6P^o)nd\ ^7P^o$$

Thus the photon is absorbed by a $4s \rightarrow 4p$ transition in the core, with the nd electron playing little part in the transition. Two large peaks are evident in these plots, associated with (a) the $^6D^o$ core state and (b) the $^6F^o$ and $^6P^o$ states (the corresponding Fe^+ target energies of the latter two states being almost identical). These PEC resonances play an important role in photoionisation from excited states of iron (Sawey and Berrington, 1990).

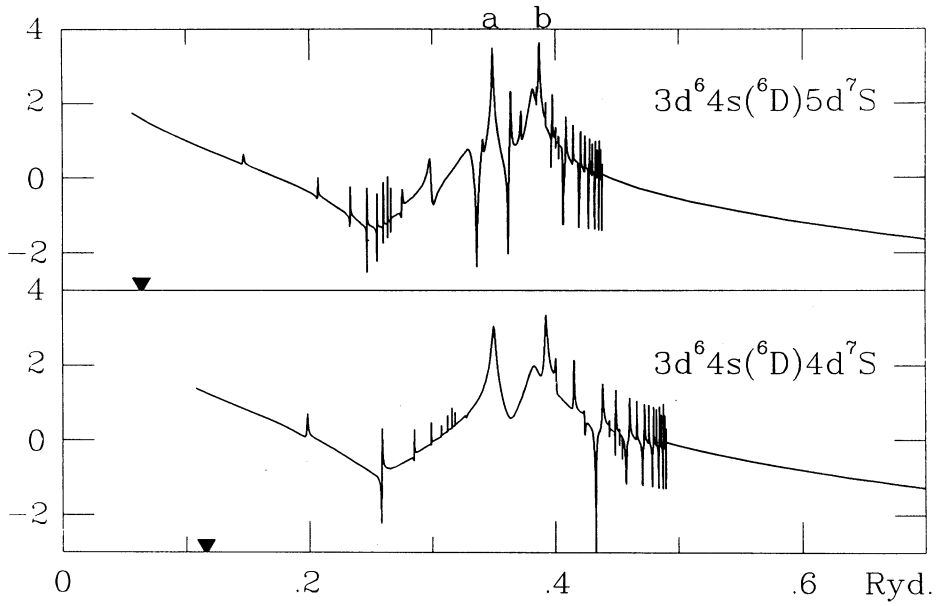

Figure 12: Log of the photoionisation cross section (in Mb) from the lowest ^7S terms of Fe as a function of photon energy (in Ryd.). Triangles mark the ionisation thresholds in each plot; *a* and *b* mark PEC resonances associated with $4s \rightarrow 4p$ core transitions: see text.

7.5 Conclusion

It is clear from the comparisons shown here that the Opacity Project calculations for Fe, although qualitatively reasonable, are not as accurate as calculations on less complex atoms and ions. Strategies to improve the accuracy would involve better Fe^+ target wavefunctions, including more target states and including relativistic effects - and would require considerably more computer resources.

Acknowledgements : Section 2. KB and CJZ are grateful to the CNRS, the DFG, MUO and OPM for financial support, computer time and hospitality. Section 4. The work was supported by a grant from the U.S. National Science Foundation (AST-8996215) and the computational work was carried out on the Cray Y-MP at the Ohio Supercomputer Center. Section 5. CM's contribution to the OP was supported by IBMV. Section 7. The computing for the Opacity Project calculation on neutral Fe was done by PMJS on a Cray Y-MP at the Ohio Supercomputer Center with the very generous help and hospitality of AKP and SNN at OSU.

References

Anders, E. and Grevesse, N., 1989, Geochim. Cosmochim. Acta **53**, 197.
Angel, G.C. and Samson, J.A.R., 1988, Phys. Rev. A **38**, 5578.
Bell, K.L., Berrington, K.A., Burke, P.G., Hibbert, A. and Kingston, A.E., 1990, J. Phys. B **23**, 2259S.
Bell, K.L., Burke, P.G., Hibbert, A. and Kingston, A.E., 1989, J. Phys. B **22**, 3197.
Bell, K.L. and Hibbert, A., 1990, J. Phys. B **23**, 2673.
Berrington, K.A., Burke, P.G., Butler, K., Seaton, M.J., Storey, P.J., Taylor, K.T. and Yu Yan, 1987, J. Phys. B **20**, 6379.
Bockasten, K. and Johansson, K.B., 1968, Ark. Phys. **37**, 563.
Bradley, D.J., Dugan, C.H., Ewart, P. and Purdie, A.F., 1976, Phys. Rev. A **13**, 1416.
Butler, K., Mendoza, C. and Zeippen, C.J., 1990, in Atomic Spectra and Oscillator Strengths for Astrophysics and Fusion Research, J.E. Hansen (Ed.), North-Holland (Amsterdam), 124.
Butler, K., Mendoza, C. and Zeippen, C.J., 1991, J. Physique IV **C1**, 135.
Butler, K. and Zeippen, C.J., 1984, Astron. Astrophys. **141**, 274.
Butler, K. and Zeippen, C.J., 1990, Astron. Astrophys. **234**, 569.
Butler, K. and Zeippen, C.J., 1991, J. Physique IV **C1**, 141.
Butler, K. and Zeippen, C.J., 1992, J. Phys. B in preparation for the ADOC series.
Cantú, A.M., Mazzoni, M., Pettini, M. and Tozzi, G.P., 1981, Phys. Rev. A **23**, 1223.
Cox, A.N. and Tabor, J.E., 1976 Astrophys. J. Suppl. Ser. **31**, 271.
Eissner, W., Jones, M. and Nussbaumer, H., 1974, Comput. Phys. Commun. **8**, 270.
Eissner, W. and Nussbaumer, H., 1969, J. Phys. B **2**, 1028.
Eissner, W. and Zeippen, C.J., 1981, J. Phys. B **14**, 2125.
Fawcett, B.C., 1975, At. Data Nucl. Data Tables **16**, 135.
Fawcett, B.C., 1984, At. Data Nucl. Data Tables **30**, 1; erratum, 1985, **33**, 479.
Fawcett, B. C., 1987, Report RAL-87-114, SERC Rutherford Appleton Laboratory, Chilton, Didcot, Oxfordshire OX11 0QX, U.K.
Froese Fischer, C. and Godefroid, M., 1982, Nucl. Instr. Meth. **202**, 307.
Fuhr, J. R., Martin, G. A. and Wiese, W. L., 1988, J. Phys. Chem. Ref. Data **17**, Supplement 4.
Glass, R., 1979, J. Phys. B. **12**, 1633.
Hibbert, A., 1974, J. Phys. B **7**, 1417.
Hibbert, A., 1975, Comp. Phys. Comm. **9**, 141.
Hibbert, A., 1980, J. Phys. B **13**, 1721.
Hibbert, A., Biémont, E., Godefroid, M. and Vaeck, N., 1991, J. Phys. B **24**, 3943.
Hibbert, A. and Hansen, J.E., 1987, J. Phys. B **20**, L245.
Hudson, R.D. and Carter, V.L., 1967, J. O. S. A. **57**, 651.
Iglesias, C.A. and Rogers, F.J., 1991, Astrophys. J. Lett. **371**, L73.
Jannitti, E., Pinzhong, F. and Tondello, G., 1986, Phys. Scr. **33**, 434.
Kohl, J.L. and Parkinson, W.H., 1973, Astrophys. J. **184**, 641.
Lang, J., Hardcastle, R.A., McWhirter, R.W.P. and Spurrett, P.H., 1987, J. Phys. B **20**, 43.

Laughlin, C., Constantinides, E.R. and Victor, G.A., 1978, J. Phys. B **11**, 2243.
Layzer, D., 1959, Ann. Phys. (NY) **8**, 271.
Le Dourneuf, M., Nahar, S.N. and Pradhan, A.K., 1992, J. Phys. B to be submitted.
Markiewicz, E., McEachran, R.P. and Cohen, M., 1981, Phys. Scr. **23**, 828.
Mendoza, C., 1990, in Atomic Spectra and Oscillator Strengths for Astrophysics and Fusion Research, J.E. Hansen (Ed.), North-Holland (Amsterdam), 126.
Mendoza, C., 1992, Lecture Notes on Physics in press.
Minnhagen, L., 1963, Ark. Phys. **25**, 203.
Moccia, R. and Spizzo, P., 1988, J. Phys. B **21**, 1133.
Moore, C.E., 1971, Atomic Energy Levels, Vol. I, NSRDS-NBS 35, US Gov. Printing Office, Washington DC.
Nicolaides, C.A., Beck D.R. and Sinanoglu, O., 1973, J. Phys. B **6**, 62.
Nussbaumer, H. and Storey, P.J., 1978, Astron. Astrophys. **64**, 139.
Reilman, R.F. and Manson, S.T., 1979, Astrophys. J. Suppl. Ser. **40**, 815.
Roig, R.A., 1975, J. Phys. B **8**, 2939.
Sampson, D.H., Clark, R.E.H. and Goett, S.J., 1981, Phys. Rev. A **24**, 2979.
Samson, J.A.R. and Angel, G.C., 1990, Phys. Rev. A **42**, 1307.
Samson, J.A.R. and Pareek, P.N., 1985, Phys. Rev. A **31**, 1470.
Sawey, P. M. J. and Berrington, K. A., 1990, J. Phys. B **23**, L817.
Sawey, P. M. J. and Berrington, K. A., 1992, J. Phys. B submitted.
Seaton, M.J., 1987, in Recent Studies in Atomic and Molecular Processes, A.E. Kingston (Ed.), Plenum Press (London), p.29.
Seaton, M.J., 1988, J. Phys. B **21**, 3033.
Seaton, M.J., 1990, J. Phys. B **23**, 3255.
Theodosiou, C.E. 1984, Phys. Rev. A **30**, 2910.
Thornbury J.F. and Hibbert, A., 1987 J. Phys. B **20**, 6447.
Tully, J.A., Le Dourneuf, M. and Zeippen, C.J., 1989, Astron. Astrophys. **211**, 485.
Tully, J.A., Seaton, M.J. and Berrington, K.A., 1990, J. Phys. B **23**, 3811.
Tully, J.A., Seaton, M.J. and Berrington, K.A., 1991, J. Physique IV **C1**, 169.
West, J.B. and Marr, G.V., 1976, Proc. R. Soc. Lond. A **349**, 397.
Yu Yan and Seaton, M.J., 1987, J. Phys. B **20**, 6409.
Yu Yan, Taylor, K.T. and Seaton, M.J., 1987, J. Phys. B **20**, 6399.
Zeippen, C.J., 1987, Astron. Astrophys. **173**, 410.
Zeippen, C.J., Butler, K. and Le Bourlot, J., 1987, Astron. Astrophys. **188**, 251.

K.A. Berrington and A. Hibbert: Department of Applied Mathematics and Theoretical Physics, The Queen's University of Belfast, Belfast BT7 1NN, Northern Ireland, UK.
C. Mendoza: IBM Venezuela Scientific Center, PO Box 64778, Caracas 1060-A, Venezuela.
A.K. Pradhan: Department of Astronomy, The Ohio State University, Columbus, Ohio 43210-1106, USA.
M.J. Seaton: Department of Physics and Astronomy, University College London, Gower Street, London WC1E 6BT, England, UK.
J.A. Tully: Observatoire de la Côte d'Azur, BP 139, 06003 Nice Cedex, France.
C.J. Zeippen: UPR 261 du CNRS et DAMAp, Observatoire de Paris, 92190 Meudon, France.